ChemComm

Enhanced 5f-δ bonding in $[U(C_7H_7)_2]^-$: Carbon K-Edge X-ray Spectroscopy, Magnetism and Electronic Structure Calculations

Journal:	*ChemComm*
Manuscript ID	CC-COM-06-2021-003414.R1
Article Type:	Communication

ChemComm

COMMUNICATION

Enhanced 5f-δ bonding in $[U(C_7H_7)_2]^-$: Carbon K-Edge X-ray Spectroscopy, Magnetism and Electronic Structure Calculations †

Received 00th January 20xx,
Accepted 00th January 20xx

DOI: 10.1039/x0xx00000x
www.rsc.org/

Yusen Qiao,[‡a] Gaurab Ganguly,[‡§b] Corwin H. Booth,[a] Jacob A. Branson,[a,c] Alexander S. Ditter,[a] Daniel J. Lussier,[a,c] Liane M. Moreau,[a] Dominic Russo,[a,c] Dumitru-Claudiu Sergentu,[b] David K. Shuh,[a] Taoxiang Sun,[a] Jochen Autschbach,*[b] and Stefan G. Minasian*[a]

5f covalency in $[U(C_7H_7)_2]^-$ was probed with carbon K-edge X-ray absorption spectroscopy (XAS) and electronic structure theory. The results revealed U 5f orbital participation in *δ*-bonding in both the ground- and core-excited states; additional 5f *ϕ*-mixing is observed in the core-excited states. Comparisons with $U(C_8H_8)_2$ show greater *δ*-covalency for $[U(C_7H_7)_2]^-$.

A deep understanding of metal-ligand interactions in f-block complexes is necessary to control their desirable physical properties and chemical reactivities and to design new separation processes, and determine environmental speciation.[1] Organometallic actinide (An) complexes containing cyclic η^n-C_nH_n ligands (n = 4–9) have been used for decades as a platform for studying fundamental aspects of metal-ligand bonding and reactivity.[1c, 2] In the case of uranocene, $U(C_8H_8)_2$, mixing between the η^8-C_8H_8 ligands and metal 5f and 6d orbitals has been confirmed both experimentally and theoretically, and today it is one of the most widely accepted examples of An–ligand covalency.[1b, 1c, 2h-l, 2n, 3] Complexes bearing two η^8-C_8H_8 ligands or substituted variants can be prepared in a range of formal oxidation states and are known for all Ln (except Pm) and most An (Th to Cm). In contrast, $[U(C_7H_7)_2]^-$ is currently the only Ln/An complex isolated experimentally with two η^8-C_7H_7 ligands, and also the only homoleptic metallocene with a formal +5 oxidation state. Clearly $[U(C_7H_7)_2]^-$ is a singular molecule, which provides a rare opportunity to explore unique aspects of chemical structure and bonding that are fundamental to the nature of all metallocenes.

The complex, [K(18-crown-6)][$U(C_7H_7)_2$], was first discovered by Ephritikhine and co-workers,[2d] as green crystals following the addition of cycloheptatriene to a mixture of tetravalent UCl_4 and K metal. A formal +5 oxidation state for the U center was assigned based on the two η^8-C_7H_7 ligands, each having –3 formal charges according to the Hückel 4n + 2 rule for aromaticity. In a subsequent theoretical study using Kohn-Sham (KS) density functional theory (DFT) calculations, Li and Bursten noted that the bonding $5f_\delta$ molecular orbitals (MOs) of e_{2u} symmetry for the $[U(C_7H_7)_2]^-$ complex have nearly equal amounts of 5f and ligand π-orbital character. Because these doubly-degenerate *δ*-bonding MOs have a combined occupation of four electrons, the authors suggested that the actual charge on the U center may be closer to +3.[2f] Subsequent electron paramagnetic resonance (EPR) measurements and crystal-field (CF) analyses support the U^{5+} oxidation state with significant metal-ligand covalent interactions.[2e] Clearly, oxidation state rules are inadequate for cases such as $[U(C_7H_7)_2]^-$, and more precise and detailed models of both 5f- and 6d-orbital interactions are needed to understand the electronic structure and its relationship to physical behavior.

Ligand K-edge X-ray absorption spectroscopy (XAS) has emerged as a powerful tool to study metal-ligand covalency, as the spectral features carry information about the coefficients of mixing between metal-centered and ligand-centered orbitals.[2h, 3b, 4] C K-edge XAS supported with time-dependent DFT (TD-DFT) and *ab initio* multireference calculations have been applied to probe the *δ*- and *ϕ*-type orbital mixing in $Th(C_8H_8)_2$ and $U(C_8H_8)_2$.[2h, 3b] Some of us showed previously by *ab initio* calculations that the ground state (GS) of $[U(C_7H_7)_2]^-$ is multiconfigurational.[2g] Under spin-orbit (SO) coupling, the GS is composed of 70% $^2\Sigma_u$ and 30% $^2\Pi_u$ (see ESI†), with strong *δ*-type covalent interactions involving the U 5f and 6d orbitals. Multi-configurational wavefunction calculations reproduced the experimentally observed $g_\parallel$ and $g_\perp$ values, whereas single-configuration DFT calculations produced an inaccurate $g_\perp$. The current study describes the C K-edge XAS of $[U(C_7H_7)_2]^-$, which provides experimental evidence of *δ*-mixing between the 5f- and ligand orbitals. *Ab initio* calculations were used to develop spectral assignments, evaluate changes in the amount of *δ*-type and *ϕ*-type covalency in the GS and core-ESs.

Before discussing the C K-edge XAS spectra in detail it is instructive to provide a framework for evaluating the orbital interactions in $[U(C_7H_7)_2]^-$. The GS electronic structure of $[U(C_7H_7)_2]^-$ has been discussed before in detail,[2e-g] and here we briefly focus on the U atomic orbitals (AOs) that form in-phase/out-of-phase combination with ligand-centered "*π*"

[a]*Chemical Sciences Division, Lawrence Berkeley National Laboratory, Berkeley, CA 94720, USA. E-mail: sgminasian@lbl.gov*
[b]*Department of Chemistry, University at Buffalo, State University of New York, Buffalo, NY 14260-3000, USA. E-mail: jochena@buffalo.edu*
[c] *Department of Chemistry, University of California, Berkeley, CA 94720, USA.*
†Electronic Supplementary Information (ESI) available: Experimental details and characterizations; computational details. See DOI: 10.1039/x0xx00000x
‡These authors contributed equally.
§Present Address: *Institute of Organic Chemistry and Biochemistry, Czech Academy of Sciences, 16610 Prague 6, Czech Republic.*

fragment orbitals (FOs, formed by C $2p_z$ AOs) that are relevant to the C K-edge XAS experiment. To simplify the following discussion, linear symmetry designations (σ, π, δ, ϕ) are used throughout, due to the (pseudo) linear symmetry of the complex. Furthermore, gerade (g) and ungerade (u) subscript labels indicate the parity with respect to the inversion center in the D_{7d} (staggered) conformer of $[U(C_7H_7)_2]^-$.

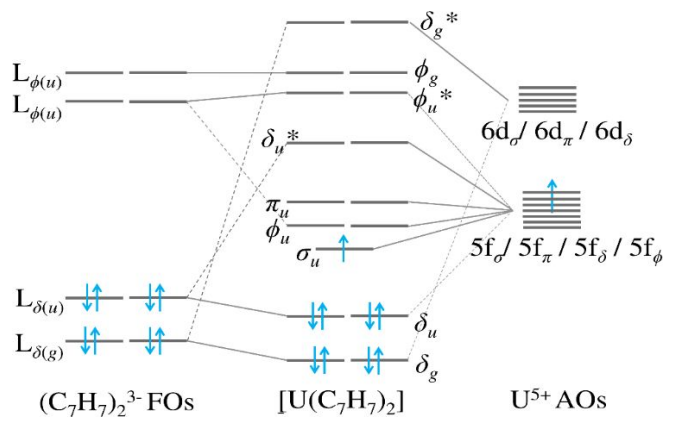

Fig. 1 Qualitative valence MO diagram for $[U(C_7H_7)_2]^-$ based on scalar relativistic (SR) DFT calculations.

Fig. 1 shows a qualitative valence MO diagram for the staggered conformer guided by DFT. The seven/five-fold degeneracy of the U 5f/6d AOs is lifted by the (pseudo) axial ligand-field into $5f_\sigma/6d_\sigma$, $5f_\pi/6d_\pi$, $5f_\delta/6d_\delta$, and $5f_\phi$ AOs. These U AOs then mix with the occupied/unoccupied $(C_7H_7)^{3-}$ FOs of matching parity and energy, labeled hereafter as L_σ, L_π, L_δ, and L_ϕ (symmetry labels added in the subscript). $L_{\delta(u)}$ and $L_{\delta(g)}$ correspond to the highest occupied ligand FOs, while $L_{\phi(u)}$ and $L_{\phi(g)}$ are the lowest unoccupied ligand FOs. Because of the larger orbital energy mismatch, mixing between the $L_{\sigma(u)}$ or $L_{\pi(u)}$ FOs (not shown in Fig. 1) and the U $5f_{\sigma(u)}$ or $5f_{\pi(u)}$ AOs, respectively, is insignificant. The resulting MOs have nearly 100% weight from the U 5f AOs and are denoted as σ_u and π_u. The U $6d_{\delta(g)}$ AOs mix more significantly with the $L_{\delta(g)}$ FOs, while the U $5f_{\delta(u)}$ AOs mix with the $L_{\delta(u)}$ FOs. This mixing results in the formation of in-phase (+, bonding) and out-of-phase (–, antibonding) MOs denoted as δ_g / δ_g^* and δ_u / δ_u^* respectively. The U $5f_{\phi(u)}$ AOs can also mix with the $L_{\phi(u)}$ FOs to form in-phase (+) and out-of-phase (–) MOs denoted as ϕ_u / ϕ_u^*. Due to symmetry restrictions, the $L_{\phi(g)}$ FOs remain purely non-bonding to the U AOs and are denoted as ϕ_g hereafter.

The magnetic susceptibility of [K(18-crown-6)][$U(C_7H_7)_2$] was measured using SQUID magnetometry (Fig. S1), which provided a μ_{eff} of 1.95 μ_B at 300 K, and 1.70 μ_B for the ground state. While this value is significantly lower than the calculated value for a free U^{5+} ion with a $^2F_{5/2}$ ground state,[5] it is well within the range commonly observed for other U^{5+} molecules[6] and in good agreement with the value of 1.78 μ_B calculated using the g values obtained using EPR by Ephritikhine and coworkers.[2e]

For C K-edge XAS, saturation and self-absorption errors that can complicate C K-edge measurements were mitigated by using a scanning transmission X-ray microscope (STXM) to obtain C K-edge XAS data from thin crystallites. According to previously established methods,[2h, 7] small droplets of [K(18-crown-6)][$U(C_7H_7)_2$] dissolved in THF were allowed to evaporate on Si_3N_4 windows in an Ar-filled glovebox. This resulted in the formation of a large number of thin crystallites in a compact area that was suitable for STXM raster scans. The background-subtracted and normalized C K-edge spectrum for [K(18-crown-6)][$U(C_7H_7)_2$] is provided in Fig. 2. Visual inspection of the pre-edge region (below *ca.* 290 eV) showed features that are—to a first approximation—indicative of excitations from core C 1s orbitals into unoccupied valence MOs associated with the $[U(C_7H_7)_2]^-$ or $[K(18\text{-crown-6})]^+$ ions.

A plot of the second derivative of the spectrum (Fig. S2) indicated that three pre-edge features are present (labeled A, B, and C in Fig. 2), however, more than three transitions are possible based on the valence MO diagram (Fig. 1). Therefore, theoretical methods were used to develop spectral assignments to understand which features were associated with the $[U(C_7H_7)_2]^-$ and $[K(18\text{-crown-6})]^+$ components.

The C K-edge spectrum was modeled by approximating the transition-dipole moments and energy differences between the many-electron states by the dipole moment integrals and orbital energy differences between the occupied and unoccupied orbitals from GS DFT calculations, to identify transitions that may be attributed to the C atoms of the $[K(18\text{-crown-6})]^+$ counter-cation instead of $[U(C_7H_7)_2]^-$. Similar C K-edge calculations have previously been performed successfully for actinide species.[8] With these approximations, the intensity of feature A in the DFT calculated spectra for the full complex [K(18-crown-6)][$U(C_7H_7)_2$] and the $[U(C_7H_7)_2]^-$ complex ion is consistent with the experimental one (Fig. 2, top). The pre- and rising-edge features of the C K-edge mainly arise from transitions into the δ_u^*, ϕ_u, ϕ_u^* of $[U(C_7H_7)_2]^-$, indicating significant U 5f mixing with ligand FOs. Additionally, there are transitions into non-bonding ligand-centered ϕ_g orbitals and less intense transitions into the 6d-based δ_g* and π_g* orbitals in

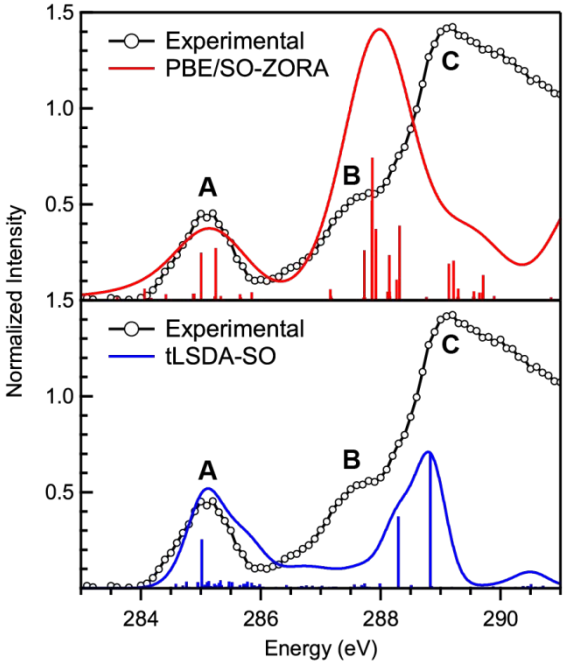

Fig. 2 Normalized C K-edge XAS spectrum obtained in transmission for [K(18-crown-6)][$U(C_7H_7)_2$] and calculated spectra for $[U(C_7H_7)_2]^-$. Top: a comparison between the experimental spectrum (black) and a spectrum modeled from DFT orbitals (red, PBE/SO-ZORA, blue-shifted by 17.1 eV to match the energy of feature A). Bottom: a comparison between the experiment (black) and multi-configurational wavefunction calculations (blue, tLSDA-SO, blue-shifted by 20.1 eV to match the energy of feature A). The vertical bars represent the energies and oscillator strengths for the individual transitions. The calculated spectral envelopes were generated with a 0.5 eV Gaussian broadening of the individual transitions.

Table 1 Assignments of final states for features A, B, and C of the C K-edge XAS spectra shown in Fig. 2, and comparison of experimental and calculated pre-edge transition energies (eV) for $[U(C_7H_7)_2]^-$

Features	NO occupation	Energies (eV)	
		XAS	tLSDA-SO[a]
GS	$(\sigma_u)^{0.70}(\pi_u)^{0.30}(\delta_u^*)^{0.00}(\phi_u)^{0.00}(\phi_u^*)^{0.00}(\phi_g)^{0.00}$	0.0	0.0
A	$(\sigma_u)^{0.76}(\pi_u)^{0.11}(\delta_u^*)^{0.23}(\phi_u)^{0.88}(\phi_u^*)^{0.01}(\phi_g)^{0.01}$	285.1	285.1
B	$(\sigma_u)^{0.47}(\pi_u)^{0.54}(\delta_u^*)^{0.22}(\phi_u)^{0.02}(\phi_u^*)^{0.45}(\phi_g)^{0.34}$	287.5	288.3
C	$(\sigma_u)^{0.75}(\pi_u)^{0.26}(\delta_u^*)^{0.16}(\phi_u)^{0.02}(\phi_u^*)^{0.45}(\phi_g)^{0.36}$	289.0	288.8

[a]Calculated tLSDA-SO energies were blue-shifted by 20.1 eV to match feature A.

the higher energy region of the rising edge. Features B and C consist of transitions based on both $[U(C_7H_7)_2]^-$ and $[K(18\text{-crown-6})]^+$ moieties, as indicated by the experimental spectrum of a reference [K(18-crown-6)]Br sample (Figs. S3-S4). As expected based on the GS orbital description above, no significant transitions were observed for the σ_u or π_u orbitals.

To describe the chemical bonding in the GS and the core-ESs with a consistent theoretical approach, multiconfigurational wavefunction calculations were conducted using the Restricted Active Space (RAS) Self Consistent Field (SCF) approach,[9] as implemented in OpenMolcas.[10] The approach for calculating XAS spectra of An species based on the RAS approach was established recently.[2g, 3b] 'Spin-free' (SF) natural orbitals (NOs) and their occupations for the SO coupled multi-configurational states were obtained as described previously.[11] Additional computational details are given in the ESI†.

The C K-edge spectrum for $[U(C_7H_7)_2]^-$, calculated within an *a posteriori* SO coupling formalism using SF RAS wavefunctions and SF energies from post-SCF multiconfigurational pair-density functional theory calculations with the 'on-top' tLSDA functional, is presented in Fig. 2, bottom. Overall, the feature energies and intensities of the pre-edge features calculated by tLSDA-SO are in good agreement with the experimental ones, apart from a slight (0.8 eV) shift to higher energy for feature B. Calculations of the transitions centered on the $[K(18\text{-crown-6})]^+$ counter cation were not feasible with the RAS approach since a much larger active space would be required. Consequently, the feature C from the RAS calculations is less intense than in the experiment, because it lacks the intensity from the countercation transitions.

The C K-edge intensities arising from $[U(C_7H_7)_2]^-$ can be further assigned in terms of the NOs of the intense core-ESs calculated with tLSDA-SO (Table 1). Isosurface plots of the δ_u^*, ϕ_u, and ϕ_g NOs of the GS and selected intense core-ESs, and their composition analysis (AO wt%), are presented in Fig. 3. Other active-space NOs are described in Fig. S7 in the ESI†. The NO analysis of the core-ES wavefunction corresponding to the most intense excitation under feature A revealed involvement of the virtual metal-centered ϕ_u and δ_u^* orbitals. The NO configuration of the most intense core-ES is $(\sigma_u)^{0.76}(\pi_u)^{0.11}(\delta_u^*)^{0.23}(\phi_u)^{0.88}(\phi_u^*)^{0.01}(\phi_g)^{0.01}$. The extent of ϕ-type orbital mixing is significant in the states corresponding to feature A, first by populating the ϕ_u orbitals, and second by causing an increased metal-ligand mixing in them as compared to the corresponding unoccupied GS orbitals (see Fig. 3). The intense core-ESs for features B and C involve ϕ_u^* and ϕ_g orbitals (see Table 1). Feature A is less intense than B and C because of comparatively low C $2p_z$ wt% in δ_u^* and ϕ_u orbitals associated with feature A. Overall, the relevant intense Core-ESs that cause features A, B, and C are all strongly multi-configurational.

The fractional occupation numbers also reflect the strong

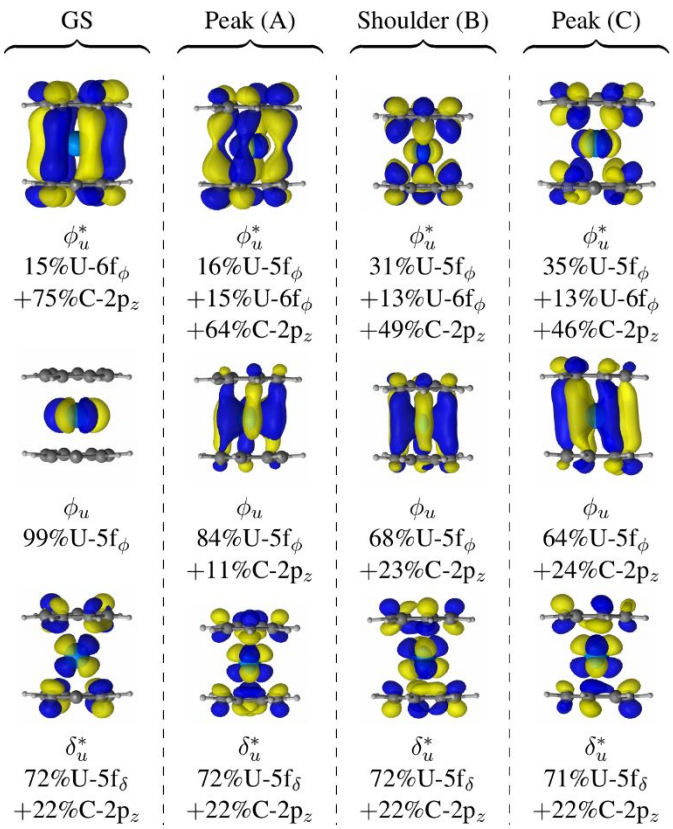

Fig. 3 Isosurfaces (±0.03 au) of ϕ_u^*, ϕ_u,and δ_u^* NOs and their decomposition in terms of AO wt% to analyze the bonding in GS and core-ESs.

multi-configurational character of the wavefunctions. For example, for feature A the σ_u occupation is increased relative to the GS, while the π_u occupation decreased, showing that this core excitation goes along with a substantial redistribution of the electron density in orbitals other than the ones that are directly implicated in the excitation. This is also the case for the electronic transitions responsible for features B and C. Specifically, the most intense transition under feature B corresponds to a core-ES with the NO configuration $(\sigma_u)^{0.47}(\pi_u)^{0.54}(\delta_u^*)^{0.22}(\phi_u)^{0.02}(\phi_u^*)^{0.45}(\phi_g)^{0.34}$. The NO occupations of the intense core-ESs attributed to features B and C differ mainly only for the metal-centered σ_u and π_u (see Table 1). However, the sum of the σ_u and π_u occupations (1.01) is the same for both features B and C.

The NO analysis of the electronic states of $[U(C_7H_7)_2]^-$ may be compared with those for $U(C_8H_8)_2$ (*cf.* Fig. S9 in the ESI†). For both metallocenes, no transitions were observed into σ_u and π_u orbitals, indicating that these orbitals are primarily U 5f AOs with little or no C 2p character. Likewise, the ϕ_u bonding orbitals for $[U(C_7H_7)_2]^-$ and $U(C_8H_8)_2$ have nearly 100% weight from the U 5f AOs and showed no significant ϕ-type covalency. However, the picture changes in the core-ESs, such that for feature A the ϕ_u orbitals are comprised of 84% U 5f and 11% C 2p character. These values are comparable to those calculated for $U(C_8H_8)_2$ (Fig. S9), where 77% U 5f and 17% C 2p character was determined for the ϕ_u orbitals in the core-ESs.

In the GS of $[U(C_7H_7)_2]^-$, the δ_u* orbitals have 72% U 5f and 22% C 2p AO wt%. These AO wt% remain unchanged, as expected, in the core-ESs for features A, B, and C. These values reflect significant δ-bonding for $[U(C_7H_7)_2]^-$, which is consistent with the previously reported EPR parameters.[2e] The C 2p AO

wt% of the δ_u* orbitals of $[U(C_7H_7)_2]^-$ is also 12% larger than that of $U(C_8H_8)_2$ (*cf.* Figs S8 and S10 in the ESI†). Since these orbitals are very similar in the GS and core-ESs of $[U(C_7H_7)_2]^-$, their composition reports on the corresponding occupied δ_u orbitals in the GS (and the core-ESs) and indicate larger δ-type covalency in $[U(C_7H_7)_2]^-$ compared to $U(C_8H_8)_2$. The trend in δ-type 5f covalent bonding may be due to several factors,[1b, 12] including the better energy match between the low energy $L_{\delta(u)}$ FOs that occurs as the 5f AOs decrease in energy with increasing oxidation state (from $U(C_8H_8)_2$ to $[U(C_7H_7)_2]^-$).

In summary, we demonstrate the use of carbon K-edge XAS and *ab initio* calculations to probe metal-ligand bonding interactions in $[U(C_7H_7)_2]^-$. The combination of experimental and theoretical results illustrates that the GS and the core-ESs relevant to the transitions in the C K-edge XAS spectra are strongly multiconfigurational. Comparisons between earlier studies on $U(C_8H_8)_2$ were derived to understand how periodic changes in An 5f AO energy impacted covalency. No significant σ- or π-orbital metal-ligand AO mixing was observed for either metallocene, whether in the GS or core-ESs. Some ϕ-type orbital mixing is observed for $[U(C_7H_7)_2]^-$ in the core-ESs but not in the GS. A comparatively large amount of δ-type orbital mixing is observed for $[U(C_7H_7)_2]^-$ in the GS and core-ESs relative to $U(C_8H_8)_2$. To explore the limits of this trend, we are currently employing C K-edge XAS to explore the covalency and the multiconfigurational character of the GSs for transuranic metallocene compounds in a range of oxidation states.

This work was supported by the Director, Office of Science, Office of Basic Energy Sciences, Division of Chemical Sciences, Geosciences, and Biosciences Heavy Element Chemistry Program of the U.S. Department of Energy (DOE) at LBNL under Contract No. DE-AC02-05CH11231. STXM research described in this paper was conducted at ALS beamline 11.0.2 supported by the Director, Office of Science, Office of Basic Energy Sciences, Division of Chemical Sciences, Geosciences, and Biosciences Condensed Phase and Interfacial Molecular Sciences Program of the U.S. DOE at LBNL under Contract No. DE-AC02-05CH11231. JA acknowledges support for the theoretical component of this study from the U.S. Department of Energy, Office of Basic Energy Sciences, Heavy Element Chemistry program, under grant DE-SC0001136. We thank the Center for Computational Research (CCR) at the University at Buffalo for providing computational resources.

Conflicts of interest

There are no conflicts to declare.

Notes and references

1. (a) G. Meyer, *The Rare Earth Elements: Fundamentals and Applications*, Wiley, Chichester, U. K., 2012; (b) M. L. Neidig, D. L. Clark and R. L. Martin, *Coord. Chem. Rev.*, 2013, **257**, 394-406; (c) M. Pepper and B. E. Bursten, *Chem. Rev.*, 1991, **91**, 719-741.
2. (a) N. Tsoureas, A. Mansikkamäki and R. A. Layfield, *Chem. Commun.*, 2020, **56**, 944-947; (b) F.-S. Guo, N. Tsoureas, G.-Z. Huang, M.-L. Tong, A. Mansikkamäki and R. A. Layfield, *Angew. Chem. Int. Ed.*, 2020, **59**, 2299-2303; (c) J. T. Miller and C. W. Dekock, *J. Organomet. Chem.*, 1981, **216**, 39-48; (d) T. Arliguie, M. Lance, M. Nierlich, J. Vigner and M. Ephritikhine, *J. Chem. Soc., Chem. Commun.*, 1995, 183-184; (e) D. Gourier, D. Caurant, T. Arliguie and M. Ephritikhine, *J. Am. Chem. Soc.*, 1998, **120**, 6084-6092; (f) J. Li and B. E. Bursten, *J. Am. Chem. Soc.*, 1997, **119**, 9021-9032; (g) D.-C. Sergentu, F. Gendron and J. Autschbach, *Chem. Sci.*, 2018, **9**, 6292-6306; (h) S. G. Minasian, J. M. Keith, E. R. Batista, K. S. Boland, D. L. Clark, S. A. Kozimor, R. L. Martin, D. K. Shuh and T. Tyliszczak, *Chem. Sci.*, 2014, **5**, 351-359; (i) A. Streitwieser and U. Mueller-Westerhoff, *J. Am. Chem. Soc.*, 1968, **90**, 7364-7364; (j) A. Streitwieser and N. Yoshida, *J. Am. Chem. Soc.*, 1969, **91**, 7528; (k) J. P. Clark and J. C. Green, *J. Organomet. Chem.*, 1976, **112**, C14-C16; (l) A. Kerridge, *Dalton Trans.*, 2013, **42**, 16428-16436; (m) A. H. H. Chang and R. M. Pitzer, *J. Am. Chem. Soc.*, 1989, **111**, 2500-2507; (n) A. Kerridge and N. Kaltsoyannis, *J. Phys. Chem. A*, 2009, **113**, 8737-8745.
3. (a) A. H. H. Chang and R. M. Pitzer, *J. Am. Chem. Soc.*, 1989, **111**, 2500-2507; (b) G. Ganguly, D.-C. Sergentu and J. Autschbach, *Chem. Eur. J.*, 2020, **26**, 1776-1788.
4. (a) T. Glaser, B. Hedman, K. O. Hodgson and E. I. Solomon, *Acc. Chem. Res.*, 2000, **33**, 859-868; (b) E. I. Solomon, B. Hedman, K. O. Hodgson, A. Dey and R. K. Szilagyi, *Coord. Chem. Rev.*, 2005, **249**, 97-129; (c) F. Frati, M. O. J. Y. Hunault and F. M. F. de Groot, *Chem. Rev.*, 2020, **120**, 4056-4110.
5. N. M. Edelstein and G. H. Lander, in *The Chemistry of the Actinide and Transactinide Elements*, eds. L. Morss, N. M. Edelstein and J. Fuger, Springer, Berlin, 3rd edn., 2006, vol. 4, ch. 20, pp. 2225-2306.
6. (a) C. R. Graves and J. L. Kiplinger, *Chem. Commun.*, 2009, 3831-3853; (b) R. K. Rosen, R. A. Andersen and N. M. Edelstein, *J. Am. Chem. Soc.*, 1990, **112**, 4588-4590; (c) S. C. Bart, C. Anthon, F. W. Heinemann, E. Bill, N. M. Edelstein and K. Meyer, *J. Am. Chem. Soc.*, 2008, **130**, 12536-12546; (d) S. Fortier, J. R. Walensky, G. Wu and T. W. Hayton, *J. Am. Chem. Soc.*, 2011, **133**, 11732-11743; (e) L. A. Seaman, G. Wu, N. Edelstein, W. W. Lukens, N. Magnani and T. W. Hayton, *J. Am. Chem. Soc.*, 2012, **134**, 4931-4940; (f) D. M. King, P. A. Cleaves, A. J. Wooles, B. M. Gardner, N. F. Chilton, F. Tuna, W. Lewis, E. J. L. McInnes and S. T. Liddle, *Nat. Commun.*, 2016, **7**; (g) C. T. Palumbo, L. Barluzzi, R. Scopelliti, I. Zivkovic, A. Fabrizio, C. Corminboeuf and M. Mazzanti, *Chem. Sci.*, 2019, **10**, 8840-8849.
7. (a) S. G. Minasian, J. M. Keith, E. R. Batista, K. S. Boland, S. A. Kozimor, R. L. Martin, D. K. Shuh, T. Tyliszczak and L. J. Vernon, *J. Am. Chem. Soc.*, 2013, **135**, 14731-14740; (b) D. E. Smiles, E. R. Batista, C. H. Booth, D. L. Clark, J. M. Keith, S. A. Kozimor, R. L. Martin, S. G. Minasian, D. K. Shuh, S. C. E. Stieber and T. Tyliszczak, *Chem. Sci.*, 2020, **11**, 2796-2809.
8. P. Å. Malmqvist, B. O. Roos and B. Schimmelpfennig, *Chem. Phys. Lett.*, 2002, **357**, 230-240.
9. (a) P. A. Malmqvist, A. Rendell and B. O. Roos, *J. Phys. Chem.*, 1990, **94**, 5477-5482; (b) J. Olsen, B. O. Roos, P. Jørgensen and H. J. A. Jensen, *J. Chem. Phys.*, 1988, **89**, 2185-2192.
10. F. Aquilante, J. Autschbach, A. Baiardi, S. Battaglia, V. A. Borin, L. F. Chibotaru, I. Conti, L. De Vico, M. Delcey, I. Fdez. Galván, N. Ferré, L. Freitag, M. Garavelli, X. Gong, S. Knecht, E. D. Larsson, R. Lindh, M. Lundberg, P. Å. Malmqvist, A. Nenov, J. Norell, M. Odelius, M. Olivucci, T. B. Pedersen, L. Pedraza-González, Q. M. Phung, K. Pierloot, M. Reiher, I. Schapiro, J. Segarra-Martí, F. Segatta, L. Seijo, S. Sen, D.-C. Sergentu, C. J. Stein, L. Ungur, M. Vacher, A. Valentini and V. Veryazov, *J. Chem. Phys.*, 2020, **152**, 214117.
11. F. Gendron, D. Páez-Hernández, F.-P. Notter, B. Pritchard, H. Bolvin and J. Autschbach, *Chem. Eur. J.*, 2014, **20**, 7994-8011.
12. (a) K. D. Warren, *Struct. Bond.*, 1977, **33**, 97-138; (b) R. G. Hayes and N. Edelstein, *J. Am. Chem. Soc.*, 1972, **94**, 8688-8691.